Chemical Science

ROYAL SOCIETY OF CHEMISTRY

EDGE ARTICLE

View Article Online
View Journal | View Issue

Cite this: *Chem. Sci.*, 2020, **11**, 3215

All publication charges for this article have been paid for by the Royal Society of Chemistry

Received 27th November 2019
Accepted 24th February 2020

DOI: 10.1039/c9sc05997k

rsc.li/chemical-science

Combination of chemotherapy and oxidative stress to enhance cancer cell apoptosis†

Xinming Li, Yanan Hou, Jintao Zhao, Jin Li, Song Wang and Jianguo Fang *

Cancer cells are vulnerable to reactive oxygen species (ROS) due to their abnormal redox environment. Accordingly, combination of chemotherapy and oxidative stress has gained increasing interest for the treatment of cancer. We report a novel seleno-prodrug of gemcitabine (**Gem**), **Se–Gem**, and evaluated its activation and biological effects in cancer cells. **Se–Gem** was prepared by introducing a 1,2-diselenolane (a five-membered cyclic diselenide) moiety into the parent drug **Gem** *via* a carbamate linker. **Se–Gem** is preferably activated by glutathione (GSH) and displays a remarkably higher potency than **Gem** (up to a 6-fold increase) to a panel of cancer cell lines. The activation of **Se–Gem** by GSH releases **Gem** and a seleno-intermediate nearly quantitatively. Unlike the most ignored side products in prodrug activation, the seleno-intermediate further catalyzes a conversion of GSH and oxygen to GSSG (oxidized GSH) and ROS *via* redox cycling reactions. Thus **Se–Gem** may be considered as a suicide agent to deplete GSH and works by a combination of chemotherapy and oxidative stress. This is the first case that employs a cyclic diselenide in prodrug design, and the success of **Se–Gem** as well as its well-defined action mechanism demonstrates that the 1,2-diselenolane moiety may serve as a general scaffold to advance constructing novel therapeutic molecules with improved potency *via* a combination of chemotherapy and oxidative stress.

Introduction

Cellular oxidizing species, generally termed reactive oxygen species (ROS), are produced in various physiological processes and are involved in many signaling pathways.[1,2] However, excessive accumulation of ROS may lead to oxidative stress that disrupts redox signaling and causes catastrophic damage to biomolecules.[3] To keep ROS at an appropriate level, cells have evolutionally adapted diverse antioxidant mechanisms, among which the glutathione system and thioredoxin system are two principal antioxidant systems in mammalian cells.[4,5] Cancer cells, due to a complex interplay of genetic aberrations and multiple misregulated signaling pathways, usually harbor elevated ROS levels compared to their benign counterparts. Accordingly, there are frequently upregulated antioxidant molecules to balance ROS and maintain a redox homeostasis in cancer cells. This abnormal redox environment of cancer cells has set a tone for ROS-mediated cancer therapy, *i.e.*, killing cancer cells by the increase of ROS production or/and inhibition of the cellular antioxidant network,[6,7] which has been supported by many successful examples.[8–13]

A general drawback of most of the conventional anticancer drugs is undesired side effects, which may be significantly reduced by the prodrug strategy. Prodrugs are inactive forms of drug molecules, and they are converted to active drugs by various endogenous or exogenous driving forces. By employing characteristic intracellular and surrounding environments of cancer cells, prodrugs that could be selectively activated by cancer cells have attracted increasing interests in the past few years.[14,15] Based on the unique microenvironment of cancer cells, a large number of prodrugs that respond to different stimuli, such as thiols,[16–19] acidic pH,[20,21] ROS,[13,22,23] enzymes,[24,25] hypoxia[26,27] and light,[28–30] have been disclosed with great success in the experimental treatment of various cancer cells. Among different types of prodrugs, exploiting the disulfide scaffold as a trigger unit has been widely adopted,[16–19,31,32] as cancer cells usually have a higher ability than normal cells to reduce the disulfide bond due to the elevated level of antioxidant molecules, such as thioredoxin (Trx), thioredoxin reductase (TrxR) and reduced glutathione (GSH).[33,34] Compared to the enormous attention on the disulfide unit in the construction of stimuli-responsive materials,[16–19,35–38] the application of the diselenide moiety has remained a Cinderella field and only limited studies have been reported.[31,39–43]

Depending on the ring size, cyclic disulfides/diselenides suffer from significant ring tension and display different

State Key Laboratory of Applied Organic Chemistry, College of Chemistry and Chemical Engineering, Lanzhou University, Lanzhou, Gansu 730000, China. E-mail: fangjg@lzu.edu.cn

† Electronic supplementary information (ESI) available: The Experimental section, original spectra (^{1}H NMR, ^{13}C NMR, and MS), purity analysis of the synthetic molecules, and some supplementary results. See DOI: 10.1039/c9sc05997k

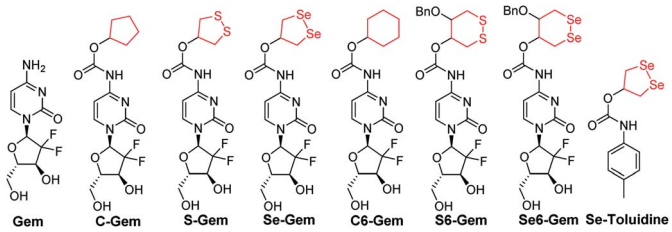

Fig. 1 Structure of the molecules used in this study.

reactivity from acyclic disulfides/diselenides.[44–47] Encouraged by the recent work on employing a cyclic disulfide moiety to construct fluorescent probes and prodrugs,[24,44,48–50] we report herein the construction of a seleno-prodrug **Se–Gem** (Fig. 1) by introducing a 1,2-diselenolane (five-membered cyclic diselenide) moiety into the anticancer drug gemcitabine (**Gem**; Fig. 1), a nucleoside analogue that has been used as a broad spectrum anticancer agent. The activation and biological effects of **Se–Gem** in cells were further evaluated. In contrast to its sulfur analogue **S–Gem**,[24] which is selectively activated by TrxR and shows lower cytotoxicity than the parent drug **Gem**, **Se–Gem** is preferably activated by GSH and has a remarkably higher cytotoxicity than **Gem** (up to a 6-fold increase). Mechanistic studies reveal that the activation of **Se–Gem** by GSH released **Gem** in a nearly quantitative manner accompanied by the formation of a seleno-intermediate. More importantly, this seleno-intermediate further catalyzed a conversion of GSH and oxygen to GSSG (oxidized GSH) and ROS *via* redox cycling reactions. A drastic alteration of the GSH/GSSG ratio was also observed in cancer cells treated with **Se–Gem**. Thus **Se–Gem** works by a combination of chemotherapy and oxidative stress, which accounts for the increased potency of **Se–Gem** compared to **Gem**. The successful construction of **Se–Gem** and clarification of its action mechanism demonstrate that the 1,2-diselenolane scaffold may serve as a general building block to advance the development of novel therapeutic molecules that combine chemotherapy and oxidative stress.

Results and discussion

Chemical synthesis

The target molecules were prepared by following the synthetic routes illustrated in Scheme 1. Hydroxy-substituted cyclic disulfides and diselenides were prepared as shown in Scheme 1A. The hydroxyl groups of **Gem** were firstly protected by reacting with *tert*-butyldimethylsilyl chloride (TBDMSCl) to provide TBS–Gem (step m, Scheme 1B), which then reacted with triphosgene and corresponding cyclic alcohols to give TBS–prodrugs (step n). The masked hydroxyl groups were released by reacting TBS–prodrugs with tetra-*n*-butylammonium fluoride (TBAF) in tetrahydrofuran (THF), affording the final prodrugs (step o). **C–Gem** and **S–Gem** were synthesized according to our previous publication.[24] The chemical structures of the prodrugs are shown in Fig. 1. The detailed synthetic procedures and characterization of compounds are described in the ESI.† Original MS spectra, NMR spectra (Fig. S4–S46†) and HPLC chromatograms are provided in the ESI (Fig. S47–S53†).

Evaluation of cytotoxicity

The cytotoxicity of different molecules to a panel of tumor cell lines was tested, and the results are summarized in Table 1. **S–Gem** was reported as a TrxR-dependent prodrug and selectively activated by TrxR. Consistent with our published results, **S–Gem** showed less cytotoxicity compared to the parent drug **Gem**.[24] Two control molecules, *i.e.*,**C–Gem** and **C6–Gem**, and **S6–Gem** were completely inactive under our experimental conditions (IC_{50} > 10 μM). As the free amine group on the dihydropyrimidine ring of **Gem** is critical for the efficacy of **Gem**,[51] the inactivation of **C–Gem**, **C6–Gem** and **S6–Gem** indicates that all of these molecules cannot be activated by the cellular environment to liberate the active drug **Gem**, which is supported by the following experiments (*vide infra*). Interestingly, **Se–Gem** showed increased cytotoxicity to all the tested cancer cells compared to **Gem**, while **Se6–Gem** had less potency than **Gem**. We also determined the cytotoxicity of **Se–Gem** to three non-cancerous cell lines (Fig. S1 in the ESI†). Interestingly, **Se–Gem**

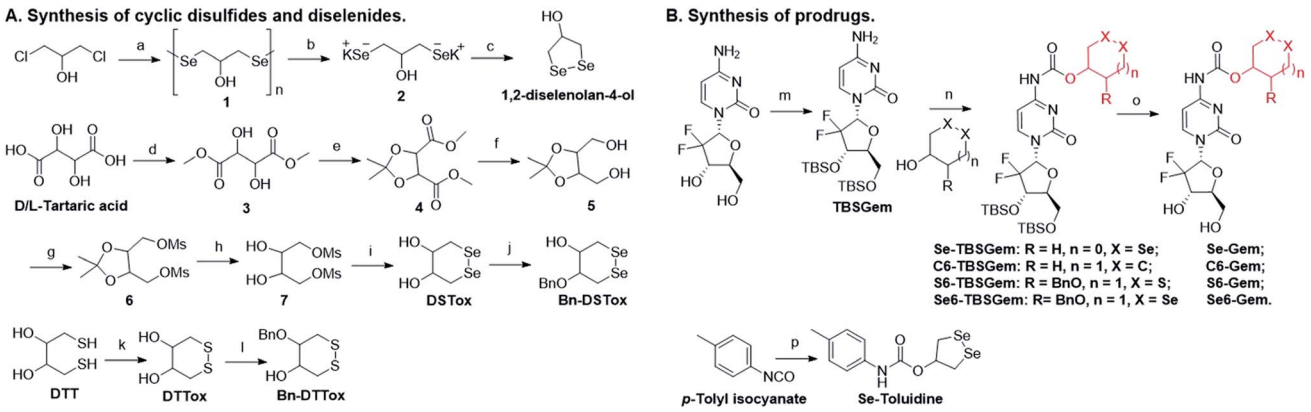

Scheme 1 Synthesis of target molecules. Reagents and conditions: (a) $N_2H_4 \cdot H_2O$, Se, and 65 °C; (b) $N_2H_4 \cdot H_2O$ and KOH; (c) HCl, 0 °C, and air; (d) $SOCl_2$ and MeOH; (e) TsOH, 2,2-dimethoxypropane, and DCM; (f) $NaBH_4$ and MeOH; (g) MSCl, Et_3N, and DCM; (h) CH_3SO_3H, EtOH, and reflux; (i) Na/naphthalene/THF and Se; (j) BnBr, KOH, 2-MeTHF, and TBAHS; (k) MeOH, KOH, and O_2; (l) BrBn, KOH, 2-MeTHF, and TBAHS; (m) imidazole, TBDMSCl, and DMF; (n) triphosgene, pyridine, and DCM; (o) TBAF and THF; (p) 1,2-diselenolan-4-ol, pyridine, and toluene.

Table 1 Cytotoxicity of **Gem** derivatives[a]

Compounds	HeLa	Hep G2	A549	7721
Gem	3.90 ± 0.41	2.46 ± 0.29	0.69 ± 0.14	0.46 ± 0.10
Se–Gem	0.88 ± 0.18**	0.47 ± 0.10**	0.11 ± 0.04**	0.33 ± 0.08*
S–Gem	6.52 ± 0.48	2.68 ± 0.31	0.85 ± 0.11	0.98 ± 0.13
Se6–Gem	>10	8.53 ± 0.56	3.84 ± 0.29	>10
C–Gem	>10	>10	>10	>10
C6–Gem	>10	>10	>10	>10
S6–Gem	>10	>10	>10	>10

[a] Compounds were incubated with cells for 96 h, and the cytotoxicity was determined by the MTT assay. The data represent the half maximal inhibitory concentration (IC_{50}) in micromolar of each compound from triplicate measurements, and are expressed as mean ± SE from triplicate measurements. *, $P < 0.05$ and **, $P < 0.01$ *vs.* the corresponding **Gem** groups.

displays decreased cytotoxicity to non-cancerous cells (the IC_{50} values for **Se–Gem** to L02 cells, HUVEC cells and 293T cells are 1.09, 2.93 and 0.45 μM, respectively).

Activation of prodrugs by GSH and TrxR

As the glutathione system and thioredoxin system are two major systems to reduce cellular disulfide bonds,[52] we then determined the activation of different molecules by GSH and TrxR. Fig. 2A shows the reduction of prodrugs by GSH. It is not convenient to determine the direct reduction of the molecules by GSH as there is no obvious change of absorbance spectra when these molecules were reduced by GSH. Thus, we adopted a coupled enzymatic assay with glutathione reductase (GR) and NADPH.[24,44] The decay of absorbance at 340 nm (A_{340}), due to the oxidation of NADPH, was monitored. Without addition of prodrugs (GSH, NADPH and GR only), the background rate of NADPH oxidation (r_{NADPH}) is 0.57 μM min^{-1} by taking 6.22 mM^{-1} cm^{-1} as the extinction coefficient of NADPH. The addition of **C–Gem**, **C6–Gem** or **S6–Gem** did not induce a significant increase of NADPH oxidation, indicating that GSH could hardly reduce them, which is consistent with the negligible cytotoxicity of these compounds (Table 1). The addition of **S–Gem** increased the rate of NADPH oxidation slightly ($r_{NADPH} = 3.37$ μM min^{-1}), suggesting that **S–Gem** is a weak substrate of GSH.[24] **Se6–Gem** was also reduced by GSH ($r_{NADPH} = 4.03$ μM min^{-1}). Strikingly, a fast oxidation of NADPH was observed when **Se–Gem** was added ($r_{NADPH} = 35.58$ μM min^{-1}), indicating that **Se–Gem** is a good substrate of GSH. The rate of **Se–Gem** reduction was also demonstrated to be dependent on GSH concentrations (Fig. 2C). Since **Se–Gem** was readily reduced by GSH, we next determined the effect of TrxR on reducing **Se–Gem**. As shown in Fig. 2B, TrxR has the ability to reduce **Se–Gem**. The addition of Trx could further increase the reduction of **Se–Gem** by TrxR, suggesting that **Se–Gem** is also a substrate of Trx. Compared to the fast reduction of **Se–Gem** by GSH ($r_{NADPH} = 35.58$ μM min^{-1}), the less efficient reduction of **Se–Gem** by TrxR/Trx ($r_{NADPH} = 7.00$ μM min^{-1}, 100 nM TrxR and 10 μM Trx) indicates that GSH plays a major role in the activation of **Se–Gem**. Consistent with our previous results, **S–Gem** was confirmed to be a good substrate of TrxR ($r_{NADPH} = 15.67$ μM min^{-1} and 50 nM TrxR).[24] The results from the reduction of different molecules by GSH and TrxR also support the conclusion in our recent work, where we comprehensively studied the reduction of cyclic disulfides and cyclic diselenides by GSH and TrxR, and disclosed that the five-membered cyclic disulfides are exclusively reduced by TrxR whereas the five-membered cyclic diselenides can be reduced by both GSH and TrxR.[44] It is worth noting that the oxidation of NADPH is not stoichiometric when **Se–Gem** is a substrate (Fig. 2A and B). We further demonstrated that oxygen in the reaction system is involved in the non-stoichiometric oxidation of NADPH, and a stoichiometric consumption of NADPH (~100 μM) upon reduction of **Se–Gem** (100 μM) was observed under anaerobic conditions (Fig. 2D). After the anaerobic oxidation of NADPH reached equilibrium (the 40–50 min period of the dotted line in Fig. 2D), the rate of NADPH

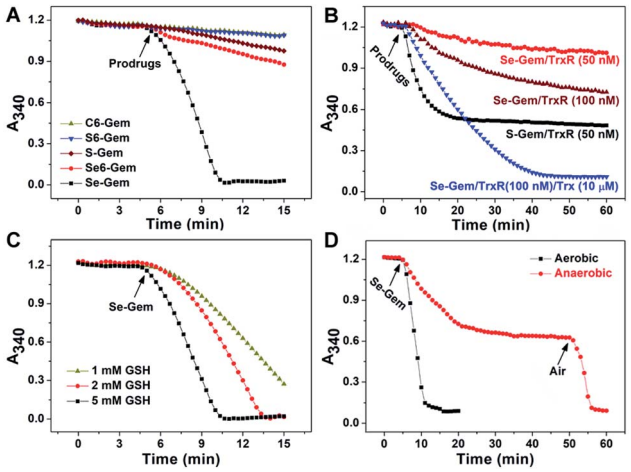

Fig. 2 Reduction of different prodrugs by GSH and TrxR/Trx. (A) Reduction of different compounds by GSH. NADPH (200 μM), GSH (5 mM) and GR (0.5 U mL^{-1}) were incubated at 37 °C in TE buffer (50 mM Tris–HCl and 1 mM EDTA, pH 7.4), and the absorbance at 340 nm was monitored. After the mixture was incubated for 5 min, compounds (100 μM) were added. (B) Reduction of **S–Gem** and **Se–Gem** by TrxR/Trx. NADPH (200 μM) and different amounts of TrxR with or without Trx were incubated at 37 °C in TE buffer, and the absorbance at 340 nm was monitored. After the mixture was incubated for 5 min, compounds (100 μM) were added. (C) Reduction of **Se–Gem** by GSH. The reaction conditions were the same as those described in (A) except that the GSH concentrations vary. (D) Aerobic and anaerobic reduction of **Se–Gem** by GSH. All experiments were performed in triplicate and the representative results are shown.

oxidation was determined to be 0.46 μM min^{-1}, quite close to the background rate of anaerobic NADPH consumption (0.30 μM min^{-1}). Further introducing air into the reaction system resumed the fast oxidation of NADPH (r_{NADPH} = 23.38 μM min^{-1}, the 50–55 min period of the dotted line in Fig. 2D).

Process of Gem release

As GSH displayed much higher efficiency in activating **Se–Gem** than did TrxR/Trx, we then determined the release of the active drug **Gem** in the presence of GSH. As shown in Fig. 3A, a gradual decrease of **Se–Gem** (retention time: 12.01 min) and increase of **Gem** (retention time: 5.87 min) were observed as the incubation time increased. The quantification of the time-dependent release of **Gem** is shown in Fig. 3B. Intriguingly, we also observed a non-stoichiometric oxidation of GSH to GSSG (retention time: 4.63 min, Fig. 3A). Under our experimental conditions, we incubated **Se–Gem** (100 μM) with GSH (5 mM) under air atmosphere, and the GSH was almost quantitatively oxidized to GSSG (~2.5 mM, Fig. 3C). This is reminiscent of the non-stoichiometric but full oxidation of NADPH (Fig. 2D). According to the activation mechanisms of the **S–Gem** prodrug by TrxR and reduction of cyclic diselenides by GSH,[24,53] we reasoned that **Se–Gem** may be activated in a similar manner to release **Gem** and a putative seleno-intermediate (Sel-Int in Scheme 2A). Selenolates are reactive and may transfer electrons to oxygen generating superoxides and selenyl radicals (Scheme 2B, eqn 1), which further dimerize to form diselenides (eqn 2). In the presence of a reducing agent, such as GSH, the selenolates are regenerated and GSH is oxidized to yield GSSG (eqn 3).[54] Taken together, selenolates catalyze the oxidation of GSH and generation of superoxides *via* redox cycling reactions under aerobic conditions (eqn 4). The proposed selenolate-catalyzed redox cycling reactions were supported by the aforementioned results, *i.e.*, non-stoichiometric oxidation of NADPH under aerobic conditions while stoichiometric oxidation of NADPH under anaerobic conditions (Fig. 2D), and non-stoichiometric oxidation of GSH under anaerobic conditions (Fig. 3C). Other biological thiols, such as Cys, can also activate **Se–Gem** in a similar manner to GSH though with less efficiency (Fig. S2 in the ESI†). As GSH is the most abundant thiol in cells, GSH is expected to play a predominant role in activating **Se–Gem** in cells.

The presence of a selenolate intermediate was further demonstrated by our recently developed specific selenolate probe Sel-green.[55] The concentration of original **Se–Gem** in the reaction mixture is 100 μM, which should generate 100 μM of Sel-Int according to Scheme 2A. A two-fold dilution of the reaction mixture of **Se–Gem** (100 μM) and GSH (5 mM) was incubated with Sel-green (10 μM) and GSH (1 mM), and the time-dependent increase of the fluorescence is shown in Fig. 4A. The inset in Fig. 4A shows the fold of fluorescence increase (F/F_0) as a function of incubation time. There is little fluorescence increment if the same reaction mixture was incubated with Sel-green without GSH (data not shown). The putative Sel-Int is not stable in air and reacts readily to form a diselenide, which may be reduced to a selenolate in the presence of a reducing agent, *e.g.*, GSH (Scheme 2B). We then quantified the selenolate in the reaction mixture of **Se–Gem** and GSH by constructing a calibration curve using the authentic diselenide compound diethyl 2,2′-diselanediyldiacetate (SeW, inset in Fig. 4B). As the concentration of SeW rose, the rate of fluorescence increment increased. The inset in Fig. 4B shows a good linearity between the concentration of SeW and the rate of fluorescence increment. Based on the calibration curve, the concentration of the selenolate in the reaction mixture could be easily obtained as 92 μM, quite close to the theoretical value (100 μM).

Since we have demonstrated the presence of a selenolate intermediate in the process of releasing **Gem** from **Se–Gem**, we then present further evidence to show the production of superoxide upon activation of **Se–Gem**. It is well known that

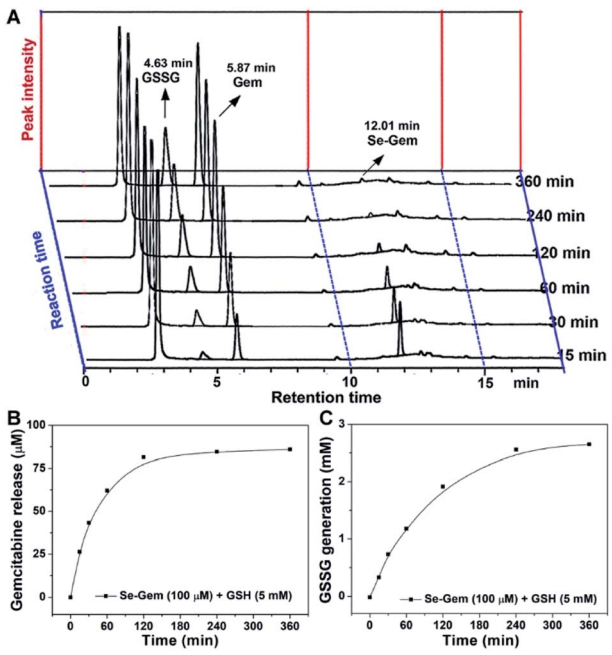

Fig. 3 GSH-mediated **Gem** release from **Se–Gem**. (A) **Se–Gem** (100 μM) was incubated with GSH (5 mM) in TE buffer at 37 °C under air conditions, and the reaction mixture was analyzed by HPLC at the indicated time points. Quantification of the time-dependent release of **Gem** and generation of GSSG is shown in (B) and (C). All experiments were performed in duplicate, and the representative results are shown.

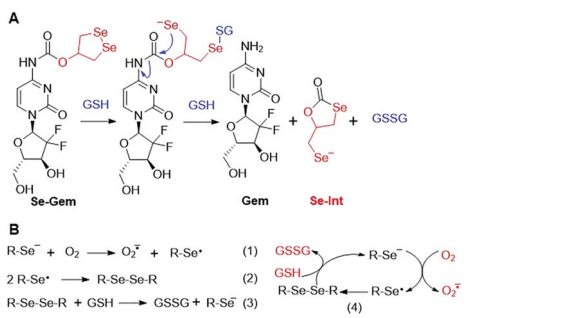

Scheme 2 (A) Activation of **Se–Gem** by GSH. (B) Redox cycling reactions of selenolate, oxygen and GSH.

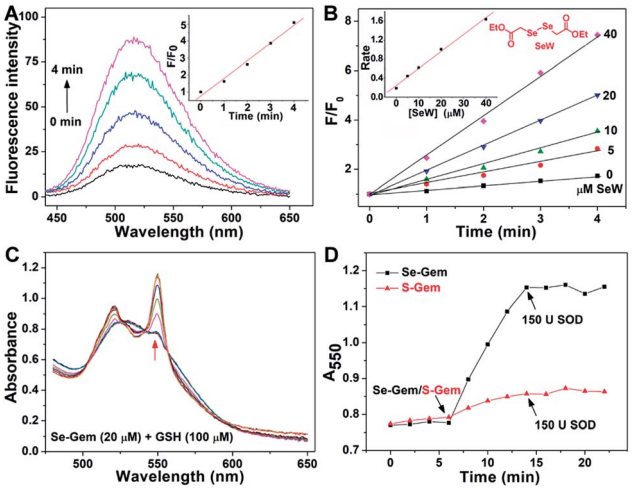

Fig. 4 Formation of a selenolate intermediate and production of superoxide in the process of GSH-mediated **Se–Gem** activation. (A) Time-dependent fluorescence increase of the reaction mixture upon incubation with additional GSH (1 mM) and the specific selenolate probe Sel-green (10 μM). The detailed conditions were described in the Experimental section. The inset shows the fold of fluorescence increase (F/F_0) as a function of incubation time. (B) Time-dependent increase of fluorescence upon incubation of Sel-green with varying concentrations of the authentic selenocompound SeW. The structure of SeW is shown. The inset shows the linear relationship of the rates of fluorescence increase and the concentrations of SeW. (C) Production of superoxide in the process of GSH-mediated **Se–Gem** reduction. GSH (100 μM) and ferric cytochrome c (1 mg mL^{-1}) were incubated in TE buffer for 6 min, and then **Se–Gem** (20 μM) was added. After the mixture was incubated for another 8 min, SOD (150 U) was added. The absorbance spectra of the reaction mixture were recorded every 2 min. (D) Time-dependent change of the absorbance at 550 nm. The experimental conditions were the same as those described in (C), and the concentration of **S–Gem** is 20 μM. All experiments were performed in triplicate, and the representative results are presented.

superoxide may reduce ferricytochrome c producing ferrocytochrome c, which has a higher absorbance at 550 nm.[56] Thus, we employed this assay to detect whether superoxide was produced in the process of **Se–Gem** activation. The incubation of **Se–Gem** with GSH generated a species that may reduce cytochrome c, which could be inhibited by further addition of superoxide dismutase (SOD) (Fig. 4C and D). This observation indicates that superoxide was produced when **Se–Gem** was incubated with GSH. In contrast, we could not detect the superoxide production by incubation of **S–Gem** with GSH (Fig. 4D). The generation of a selenolate intermediate and superoxide supports the proposed mechanism of **Se–Gem** activation by GSH (Scheme 2) and accounts for the observed non-stoichiometric oxidation of NADPH (Fig. 2) and GSH (Fig. 3) under aerobic conditions. The cellular SOD may then convert the superoxide to long-lived and cell membrane-permeable hydrogen peroxide (H_2O_2) that further contributes to oxidative stress.

To further examine the contribution of **Gem** and the diselenide unit to the observed cytotoxicity of **Se–Gem**, we further compared the cytotoxicity of **Se–Gem**, **Gem** and Se–toluidine. Fig. S3 (in the ESI†) shows clearly that Se–toluidine has much less toxicity to all the tested cell lines than does **Se–Gem**. This result further supports the fact that the cytotoxicity of **Se–Gem** is not solely caused by the cyclic diselenide unit, and both **Gem** and the diselenide unit contribute to the increased cytotoxicity of **Se–Gem**. In addition, as the incorporation of a strained cyclic disulfide/diselenide moiety into a target molecule could also improve the molecule's membrane permeability,[45–47] **Se–Gem** may be taken up by cells more easily than **Gem** itself, which could also contribute to the increased cytotoxicity of **Se–Gem**.

Induction of oxidative stress and apoptosis

The biological functions of **Se–Gem** were further studied. The treatment of Hep G2 cells with **Se–Gem** caused a dose-dependent decrease of the GSH/GSSG ratio and the total cellular thiols (Fig. 5A and B). Although the treatment of the cells with **S–Gem** also led to a significant decrease of the GSH/GSSG ratio and the total cellular thiols, the effect of **Se–Gem** was much more pronounced. The treatment of the cells with **Gem** gave a slight decrease of the GSH/GSSG ratio, but has a marginal effect on the total cellular thiols. We also determined the cellular ROS level upon treatment with different molecules. Two ROS probes, *i.e.*, a general ROS probe 2′,7′-dichlorofluorescein diacetate (DCFH-DA) and a specific superoxide probe dihydroethidium (DHE), were employed. As shown in Fig. 5C and D, **Se–Gem** induced the accumulation of ROS and superoxide in the cells. However, neither **S–Gem** nor **Gem** caused the elevation of ROS or superoxide under the same experimental conditions. Taken together, the treatment of Hep G2 cells with **Se–Gem** causes oxidative stress. Resistance to apoptosis is a general hallmark of malignant cells, which is caused by a complex interplay of genetic mutations and various misregulated signaling pathways. We next determined whether **Se–Gem** could induce apoptotic cell death of Hep G2 cells by the fluorescein isothiocyanate (FITC)-labeled Annexin V (Annexin V-FITC) and propidium iodide (PI) double staining assay. The scatter plots representing the distribution of live cells, apoptotic cells and necrotic cells are shown in Fig. 6A–D, and the quantification of the cell distribution is shown in Fig. 6E. The treatment of the cells with increasing concentrations of **Se–Gem** induced an increasing number of apoptotic cells, while the number of necrotic cells among all the cells remained small. Thus, **Se–Gem** predominantly induces apoptotic cell death of Hep G2 cells.

Chemotherapy, *e.g.*, treatment of cancer by using drugs to kill cancer cells, remains an important way to deal with cancer and may be the only treatment to the patients with metastasized tumors. Elevated generation of ROS and an altered redox homeostasis have long been observed in various types of cancer cells, and this abnormal redox environment has been harnessed to kill cancer cells by imposing extra ROS on them through promoting the cellular ROS production or/and inhibiting the cellular antioxidant system.[2,7] Accordingly, the combination of chemotherapy and ROS has gained increasing interest to improve the anticancer effect of chemotherapeutic drugs.[21,57–60] To maintain a constant production of ROS, quinones, due to their characteristic redox properties, have been applied to construct prodrugs by employing the reducing equivalent

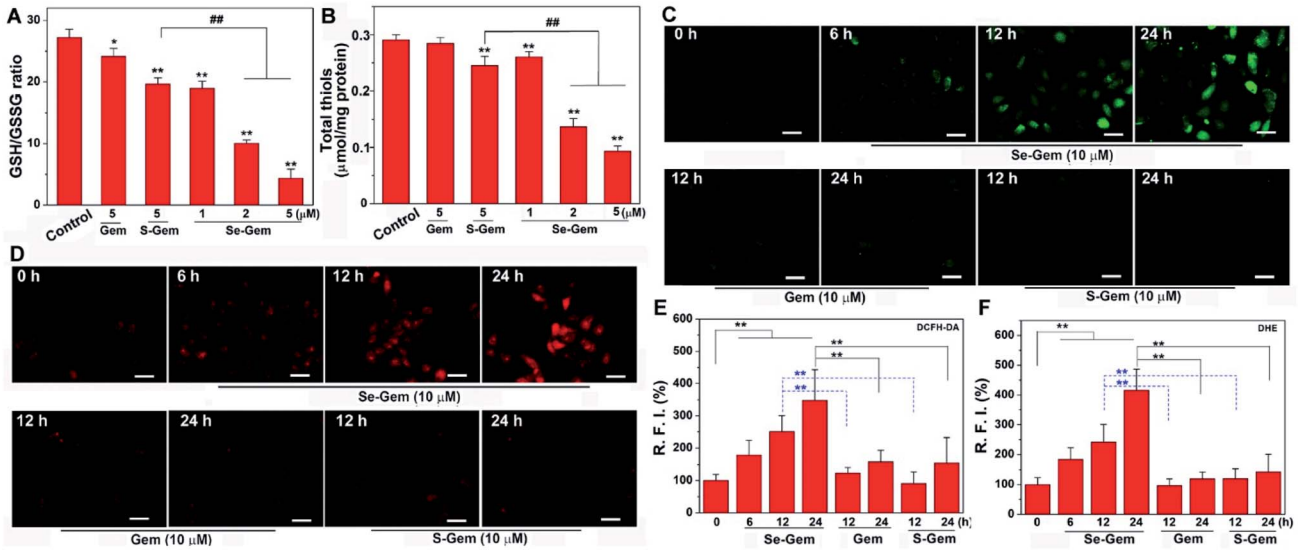

Fig. 5 Induction of oxidative stress by **Se–Gem**. (A) Alteration of the GSH/GSSG ratio in Hep G2 cells upon treatment with different compounds. The cells were treated with indicated compounds for 72 h, and the intracellular GSH/GSSG ratio was determined. (B) Alteration of total cellular thiols in Hep G2 cells upon treatment with different compounds. The cells were treated with indicated compounds for 72 h, and the cellular total thiols were determined. (C) Accumulation of ROS in Hep G2 cells upon **Se–Gem** treatment. The cells were treated with different compounds for the indicated times, and the cellular ROS level was determined by DCFH-DA staining. (D) Accumulation of superoxide in Hep G2 cells upon **Se–Gem** treatment. The cells were treated with different compounds for the indicated times, and the cellular superoxide level was determined by DHE staining. Scale bars = 25 μm. Quantification results of the relative fluorescence intensity (RFI) in individual cells by ImageJ are shown in (E) and (F). All experiments were performed in triplicate. The representative results for (C) and (D) are shown, and others are presented as mean ± SE. In (A) and (B), the control groups were treated without drugs but with the same amount of DMSO (0.1%, v/v). *, $P < 0.05$ and **, $P < 0.01$ *vs.* the control groups, and $^{\#\#} < 0.01$ among different groups. In (E) and (F), **, $P < 0.01$ among different groups.

NAD(P)H in the catalysis of NAD(P)H quinone oxidoreductase 1 (NQO1).[59,60] We presented in this work that the redox properties of selenolates could also be harnessed to construct prodrugs that work *via* combination of chemotherapy and oxidative stress. In contrast to quinones, which utilize NAD(P)H and NQO1 as reducing partners, selenolates are readily coupled with GSH and oxygen to generate GSSG and superoxides. **Se–Gem** was prepared by conjugation of the 1,2-diselenolane unit to the anticancer drug **Gem** and displayed enhanced potency in comparison with the parent **Gem**. Further extensive studies revealed that the conjugate **Se–Gem** was activated predominantly by GSH to release **Gem**. More importantly, the seleno-intermediate generated in the process of **Se–Gem** activation catalyzed the suicide oxidation of GSH accompanied by a constant production of ROS. As the most abundant antioxidant molecule in live cells, GSH is frequently upregulated in cancer cells and essential for the fast proliferation of cancer cells.[4,34,61] Thus, targeting GSH inhibition has been considered as an effective way to kill cancer cells.[8,62] The release of the active drug **Gem** and conversion of the antioxidant GSH to ROS account for the enhanced cytotoxicity of **Se–Gem**. The accumulation of GSSG and ROS was also observed in the Hep G2 cells treated with **Se–Gem**. We also demonstrated that the cytotoxicity of **Se–Gem** was mediated by its ability to induce apoptosis. The successful construction of **Se–Gem** suggests that the conjugation of the 1,2-diselenolane scaffold to anticancer drugs may be a general strategy to prepare novel therapeutic agents with improved potency.

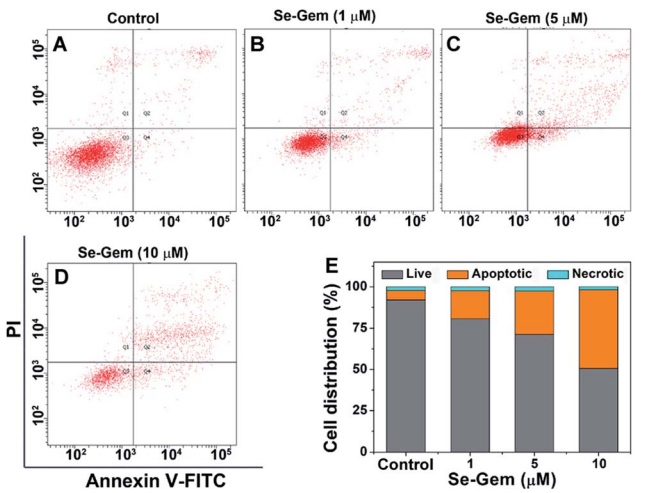

Fig. 6 Induction of apoptosis by **Se–Gem**. (A)–(D) Hep G2 cells were treated with **Se–Gem** for 48 h, and the apoptotic cell death was evaluated by the Annex V-FITC/PI double staining assay. The control groups were treated without drugs but with the same amount of DMSO (0.1%, v/v). (E) Quantification of live cells, apoptotic cells and necrotic cells from the scatter plots (A)–(D). All experiments were performed in triplicate, and the representative results are shown.

Conclusions

In summary, we present a novel strategy with a well-defined mechanism to construct therapeutic agents that combine chemotherapy and oxidative stress to kill cancer cells. The conjugation of a 1,2-diselenolane unit to **Gem** affords **Se–Gem**,

which has enhanced potency compared to the parent drug **Gem**. Further mechanistic studies reveal that **Se–Gem** is preferably activated by the cellular GSH to liberate the active drug **Gem** and causes a suicide oxidation of GSH with a simultaneous generation of ROS. Consequently, **Se–Gem** displayed an improved potency to induce the apoptosis of cancer cells.

Conflicts of interest

The authors declare no competing financial interest.

Acknowledgements

Financial supports from the National Natural Science Foundation of China (21778028 & 21572093), the Natural Science Foundation of Gansu Province (18JR4RA003), and the 111 project are acknowledged.

References

1 C. R. Reczek and N. S. Chandel, *Curr. Opin. Cell Biol.*, 2015, **33**, 8–13.
2 K. M. Holmstrom and T. Finkel, *Nat. Rev. Mol. Cell Biol.*, 2014, **15**, 411–421.
3 H. Sies, C. Berndt and D. P. Jones, *Annu. Rev. Biochem.*, 2017, **86**, 715–748.
4 E. Hatem, N. El Banna and M. E. Huang, *Antioxid. Redox Signaling*, 2017, **27**, 1217–1234.
5 J. Lu and A. Holmgren, *Free Radical Biol. Med.*, 2014, **66**, 75–87.
6 M. Hornsveld and T. B. Dansen, *Antioxid. Redox Signaling*, 2016, **25**, 300–325.
7 D. Trachootham, J. Alexandre and P. Huang, *Nat. Rev. Drug Discovery*, 2009, **8**, 579–591.
8 H. Ogiwara, K. Takahashi, M. Sasaki, T. Kuroda, H. Yoshida, R. Watanabe, A. Maruyama, H. Makinoshima, F. Chiwaki, H. Sasaki, T. Kato, A. Okamoto and T. Kohno, *Cancer Cell*, 2019, **35**, 177–190.
9 X. Sun, W. Wang, J. Chen, X. Cai, J. Yang, Y. Yang, H. Yan, X. Cheng, J. Ye, W. Lu, C. Hu, H. Sun, J. Pu and P. Cao, *Cancer Res.*, 2017, **77**, 926–936.
10 L. Leanza, M. Romio, K. A. Becker, M. Azzolini, L. Trentin, A. Manago, E. Venturini, A. Zaccagnino, A. Mattarei, L. Carraretto, A. Urbani, S. Kadow, L. Biasutto, V. Martini, F. Severin, R. Peruzzo, V. Trimarco, J. H. Egberts, C. Hauser, A. Visentin, G. Semenzato, H. Kalthoff, M. Zoratti, E. Gulbins, C. Paradisi and I. Szabo, *Cancer Cell*, 2017, **31**, 516–531.
11 I. S. Harris, A. E. Treloar, S. Inoue, M. Sasaki, C. Gorrini, K. C. Lee, K. Y. Yung, D. Brenner, C. B. Knobbe-Thomsen, M. A. Cox, A. Elia, T. Berger, D. W. Cescon, A. Adeoye, A. Brustle, S. D. Molyneux, J. M. Mason, W. Y. Li, K. Yamamoto, A. Wakeham, H. K. Berman, R. Khokha, S. J. Done, T. J. Kavanagh, C. W. Lam and T. W. Mak, *Cancer Cell*, 2015, **27**, 211–222.
12 D. Trachootham, Y. Zhou, H. Zhang, Y. Demizu, Z. Chen, H. Pelicano, P. J. Chiao, G. Achanta, R. B. Arlinghaus, J. Liu and P. Huang, *Cancer Cell*, 2006, **10**, 241–252.
13 J. Noh, B. Kwon, E. Han, M. Park, W. Yang, W. Cho, W. Yoo, G. Khang and D. Lee, *Nat. Commun.*, 2015, **6**, 6907.
14 M. H. Lee, A. Sharma, M. J. Chang, J. Lee, S. Son, J. L. Sessler, C. Kang and J. S. Kim, *Chem. Soc. Rev.*, 2018, **47**, 28–52.
15 X. Zhang, X. Li, Q. You and X. Zhang, *Eur. J. Med. Chem.*, 2017, **139**, 542–563.
16 M. Ye, X. Wang, J. Tang, Z. Guo, Y. Shen, H. Tian and W. H. Zhu, *Chem. Sci.*, 2016, **7**, 4958–4965.
17 M. H. Lee, E. J. Kim, H. Lee, H. M. Kim, M. J. Chang, S. Y. Park, K. S. Hong, J. S. Kim and J. L. Sessler, *J. Am. Chem. Soc.*, 2016, **138**, 16380–16387.
18 F. Kong, Z. Liang, D. Luan, X. Liu, K. Xu and B. Tang, *Anal. Chem.*, 2016, **88**, 6450–6456.
19 X. Wu, X. Sun, Z. Guo, J. Tang, Y. Shen, T. D. James, H. Tian and W. Zhu, *J. Am. Chem. Soc.*, 2014, **136**, 3579–3588.
20 A. Fernandez, M. Vermeren, D. Humphries, R. Subiros-Funosas, N. Barth, L. Campana, A. MacKinnon, Y. Feng and M. Vendrell, *ACS Cent. Sci.*, 2017, **3**, 995–1005.
21 J. Song, L. Lin, Z. Yang, R. Zhu, Z. Zhou, Z. W. Li, F. Wang, J. Chen, H. Yang and X. Chen, *J. Am. Chem. Soc.*, 2019, **141**, 8158–8170.
22 R. Kumar, J. Han, H. J. Lim, W. X. Ren, J. Y. Lim, J. H. Kim and J. S. Kim, *J. Am. Chem. Soc.*, 2014, **136**, 17836–17843.
23 T. T. Hoang, T. P. Smith and R. T. Raines, *Angew. Chem., Int. Ed.*, 2017, **56**, 2619–2622.
24 X. Li, Y. Hou, X. Meng, C. Ge, H. Ma, J. Li and J. Fang, *Angew. Chem., Int. Ed.*, 2018, **57**, 6141–6145.
25 X. Jia, Y. Zhang, Y. Zou, Y. Wang, D. Niu, Q. He, Z. Huang, W. Zhu, H. Tian, J. Shi and Y. Li, *Adv. Mater.*, 2018, **30**, e1704490.
26 D. Cui, J. Huang, X. Zhen, J. Li, Y. Jiang and K. Pu, *Angew. Chem., Int. Ed.*, 2019, **58**, 5920–5924.
27 P. Verwilst, J. Han, J. Lee, S. Mun, H. G. Kang and J. S. Kim, *Biomaterials*, 2017, **115**, 104–114.
28 V. H. van Rixel, V. Ramu, A. B. Auyeung, N. Beztsinna, D. Y. Leger, S. T. Hilt, S. E. Le Devedec, T. Yildiz, T. Betancourt, B. Gildner, T. W. Hudnall, V. Sol, B. Liagre, A. Kornienko and S. Bonnet, *J. Am. Chem. Soc.*, 2019, **141**, 18444–18454.
29 D. W. Zheng, Y. Chen, Z. H. Li, L. Xu, C. X. Li, B. Li, J. X. Fan, S. X. Cheng and X. Z. Zhang, *Nat. Commun.*, 2018, **9**, 1680.
30 X. Q. Wang, F. Gao and X. Z. Zhang, *Angew. Chem., Int. Ed.*, 2017, **56**, 9029–9033.
31 B. Sun, C. Luo, X. Zhang, M. Guo, M. Sun, H. Yu, Q. Chen, W. Yang, M. Wang, S. Zuo, P. Chen, Q. Kan, H. Zhang, Y. Wang, Z. He and J. Sun, *Nat. Commun.*, 2019, **10**, 3211.
32 C. Yan, Z. Guo, Y. Shen, Y. Chen, H. Tian and W. H. Zhu, *Chem. Sci.*, 2018, **9**, 4959–4969.
33 J. Zhang, X. Li, X. Han, R. Liu and J. Fang, *Trends Pharmacol. Sci.*, 2017, **38**, 794–808.
34 J. M. Estrela, A. Ortega and E. Obrador, *Crit. Rev. Clin. Lab. Sci.*, 2006, **43**, 143–181.
35 H. Jia, G. Hu, D. Shi, L. Gan, H. Zhang, X. Yao and J. Fang, *Anal. Chem.*, 2019, **91**, 8524–8531.

36 J. Fu, C. Yu, L. Li and S. Q. Yao, *J. Am. Chem. Soc.*, 2015, **137**, 12153–12160.
37 M. H. Lee, Z. Yang, C. W. Lim, Y. H. Lee, S. Dongbang, C. Kang and J. S. Kim, *Chem. Rev.*, 2013, **113**, 5071–5109.
38 P. Yuan, X. Mao, X. Wu, S. S. Liew, L. Li and S. Q. Yao, *Angew. Chem., Int. Ed.*, 2019, **58**, 7657–7661.
39 Z. Lou, P. Li, X. Sun, S. Yang, B. Wang and K. Han, *Chem. Commun.*, 2013, **49**, 391–393.
40 S. T. Manjare, S. Kim, W. D. Heo and D. G. Churchill, *Org. Lett.*, 2014, **16**, 410–412.
41 X. Han, F. Yu, X. Song and L. Chen, *Chem. Sci.*, 2016, **7**, 5098–5107.
42 X. Han, X. Song, F. Yu and L. Chen, *Chem. Sci.*, 2017, **8**, 6991–7002.
43 X. He, J. Zhang, C. Li, Y. Zhang, Y. Lu, Y. Zhang, L. Liu, C. Ruan, Q. Chen, X. Chen, Q. Guo, T. Sun, J. Cheng and C. Jiang, *Theranostics*, 2018, **8**, 4884–4897.
44 X. Li, B. Zhang, C. Yan, J. Li, S. Wang, X. Wei, X. Jiang, P. Zhou and J. Fang, *Nat. Commun.*, 2019, **10**, 2745.
45 N. Chuard, A. I. Poblador-Bahamonde, L. Zong, E. Bartolami, J. Hildebrandt, W. Weigand, N. Sakai and S. Matile, *Chem. Sci.*, 2018, **9**, 1860–1866.
46 D. Abegg, G. Gasparini, D. G. Hoch, A. Shuster, E. Bartolami, S. Matile and A. Adibekian, *J. Am. Chem. Soc.*, 2017, **139**, 231–238.
47 E. Bartolami, D. Basagiannis, L. Zong, R. Martinent, Y. Okamoto, Q. Laurent, T. R. Ward, M. Gonzalez-Gaitan, N. Sakai and S. Matile, *Chem.–Eur. J.*, 2019, **25**, 4047–4051.
48 F. Kong, Y. Zhao, Z. Liang, X. Liu, X. Pan, D. Luan, K. Xu and B. Tang, *Anal. Chem.*, 2017, **89**, 688–693.
49 L. Zhang, D. Duan, Y. Liu, C. Ge, X. Cui, J. Sun and J. Fang, *J. Am. Chem. Soc.*, 2014, **136**, 226–233.
50 G. Butora, N. Qi, W. Fu, T. Nguyen, H. C. Huang and I. W. Davies, *Angew. Chem., Int. Ed.*, 2014, **53**, 14046–14050.
51 J. T. Weiss, J. C. Dawson, C. Fraser, W. Rybski, C. Torres-Sanchez, M. Bradley, E. E. Patton, N. O. Carragher and A. Unciti-Broceta, *J. Med. Chem.*, 2014, **57**, 5395–5404.
52 C. G. Miller, A. Holmgren, E. S. J. Arner and E. E. Schmidt, *Free Radical Biol. Med.*, 2018, **127**, 248–261.
53 Q. Laurent, N. Sakai and S. Matile, *Helv. Chim. Acta*, 2019, **102**, e1800209.
54 C. W. Nogueira, G. Zeni and J. B. Rocha, *Chem. Rev.*, 2004, **104**, 6255–6285.
55 B. Zhang, C. Ge, J. Yao, Y. Liu, H. Xie and J. Fang, *J. Am. Chem. Soc.*, 2015, **137**, 757–769.
56 T. Liu, J. Zhang, X. Han, J. Xu, Y. Wu and J. Fang, *Free Radical Biol. Med.*, 2019, **135**, 216–226.
57 S. Wang, G. Yu, Z. Wang, O. Jacobson, L. S. Lin, W. Yang, H. Deng, Z. He, Y. Liu, Z. Y. Chen and X. Chen, *Angew. Chem., Int. Ed.*, 2019, **58**, 14758–14763.
58 W. Zhang, X. Hu, Q. Shen and D. Xing, *Nat. Commun.*, 2019, **10**, 1704.
59 S. Wang, Z. Wang, G. Yu, Z. Zhou, O. Jacobson, Y. Liu, Y. Ma, F. Zhang, Z. Y. Chen and X. Chen, *Adv. Sci.*, 2019, **6**, 1801986.
60 X. Huang, E. A. Motea, Z. R. Moore, J. Yao, Y. Dong, G. Chakrabarti, J. A. Kilgore, M. A. Silvers, P. L. Patidar, A. Cholka, F. Fattah, Y. Cha, G. G. Anderson, R. Kusko, M. Peyton, J. Yan, X. J. Xie, V. Sarode, N. S. Williams, J. D. Minna, M. Beg, D. E. Gerber, E. A. Bey and D. A. Boothman, *Cancer Cell*, 2016, **30**, 940–952.
61 E. Desideri, F. Ciccarone and M. R. Ciriolo, *Nutrients*, 2019, **11**, E1926.
62 M. Zarei, H. Du, A. H. Nassar, R. E. Yan, K. Giannikou, S. H. Johnson, H. C. Lam, E. P. Henske, Y. Wang, T. Zhang, J. Asara and D. J. Kwiatkowski, *J. Exp. Med.*, 2019, **216**, 2635–2652.